Journal of Dental Sciences 20 (2025) 178–188

Available online at www.sciencedirect.com

ScienceDirect

journal homepage: www.e-jds.com

Original Article

Improving osteogenic properties of zirconia ceramic via glow discharge plasma-enhanced deposition of amine organic compound

Lwin Moe Aung [a], Ting-Yi Renn [a], Jerry Chin-Yi Lin [a,b], Eisner Salamanca [a], Yi-Fan Wu [a,c], Yu-Hwa Pan [a,d,e], Nai-Chia Teng [a,f], Haw-Ming Huang [a], Ying-Sui Sun [g*], Wei-Jen Chang [a,h**]

[a] School of Dentistry, College of Oral Medicine, Taipei Medical University, Taipei, Taiwan
[b] Department of Oral Medicine, Infection and Immunity, Harvard School of Dental Medicine, Boston, MA, United States
[c] Department of Biomedical Engineering, Ming-Chuan University, Taoyuan, Taiwan
[d] Department of Dentistry, Chang Gung Memorial Hospital, Taipei, Taiwan
[e] School of Dentistry, College of Medicine, China Medical University, Taichung, Taiwan
[f] Department of Dentistry, Taipei Medical University Hospital, Taipei, Taiwan
[g] School of Dental Technology, College of Oral Medicine, Taipei Medical University, Taipei, Taiwan
[h] Dental Department, Shuang-Ho Hospital, Taipei Medical University, New Taipei City, Taiwan

Received 7 August 2024; Final revision received 17 August 2024
Available online 29 August 2024

KEYWORDS
Allylamine;
Argon glow discharge plasma (GDP) treatment;
Surface modification;
Zirconia

Abstract *Background/purpose:* Osseointegration potential is greatly depended on the interaction between bone cells and dental implant surface. Since zirconia ceramic has a bioinert surface, functionalization of the surface with an organic compound allylamine was conducted to overcome its drawback of minimal interaction with the surrounding bone.
Materials and methods: The zirconia surface was initially treated with argon glow discharge plasma (GDP), then combined with amine plasma at three different conditions of 50-W, 75-W and 85-W, to prepare the final samples. The surface characteristics and cell biocompatibility were then evaluated.
Results: Surface morphology analysis revealed a bulbous pattern on allylamine-treated sample groups. The aromatic C–H, C–O, N–H, C^C, and C–H stretching and functional groups have been identified. Surface roughness increased, and hydrophilicity improved after surface

* Corresponding author. School of Dental Technology, College of Oral Medicine, Taipei Medical University, No. 250, Wu-Hsing Street, Xinyi District, Taipei city 110, Taiwan.
** Corresponding author. School of Dentistry, College of Oral Medicine, Taipei Medical University, No. 250, Wu-Hsing Street, Xinyi District, Taipei city 110, Taiwan.
E-mail addresses: yingsuisun@tmu.edu.tw (Y.-S. Sun), cweijen1@tmu.edu.tw (W.-J. Chang).

https://doi.org/10.1016/j.jds.2024.08.011

modification. Cell viability analysis showed the highest result for the allylamine 50-W (A50) group. Alkaline phosphatase (ALP) assay indicated the A50 group had the highest activity, subsequently promoting late-stage mineralization at day 21. The reverse transcription-quantitative polymerase chain reaction (RT-qPCR) data demonstrated a significant upregulation of osteogenic gene expressions from day 1 to day 21.

Conclusion: The allylamine-treated surface demonstrates immense enhancement in the surface hydrophilicity as well as in the viability, differentiation, and osteogenic properties of osteoblast-like cells. This makes it a promising candidate for future dental implant applications.

Introduction

Dental implants have been extensively employed in dental implantology and orthopaedic surgery for various purposes, including facilitating fracture healing, addressing skeletal anomalies, and replacing damaged teeth and joints.[1] Although titanium is commonly utilized as the primary material for manufacturing implants, it has some disadvantages, such as dissemination of its particles into the oral environment and aesthetic concern.[2] Therefore, zirconia was introduced to solve this problem and is currently regarded as the second most commonly utilized material after titanium.

Yttria-stabilized tetragonal zirconia polycrystal (Y-TZP) is a promising dental implant material undergoing extensive research.[3] This zirconium oxide exhibits enhanced mechanical characteristics, including a flexural strength of 900 MPa, fracture toughness up to 10 MPa$\sqrt{m}$, high bending strength, and resistance to corrosion and chemical stability.[4] Moreover, several studies have illustrated that zirconia can reduce bacterial adhesion and biofilm accumulation, thereby lowering the risk of inflammatory reactions.[5] Despite these encouraging results, long-term outcomes are still lacking, and challenges related to zirconia osseointegration need to be addressed.

Current research on surface treatments for zirconia implants mainly includes sandblasting and acid etching, laser treatment, powder injection molded (PIM), and sintering.[6,7] However, these treatment techniques can negatively impact zirconia's mechanical strength. For instance, residual stress from sandblasting may weaken the material,[8] and heat treatment can reduce its biaxial flexural strength.[9] To address these issues, researchers have endeavored to alter the surface of the material without compromising its physical properties. In our study, we present a low-temperature glow discharge plasma (GDP) treatment combined with amine organic compounds to obtain a bioactive ceramic implant material that enhances interaction with bone cells.

GDP treatment is widely used for sterilizing and modifying surface characteristics of biomaterials by employing low atmospheric pressure and low thermal plasma to form functional proteins.[10] This procedure facilitated the surface modification of biodegradable polymers while preserving their inherent characteristics.[11] Combining GDP treatment with allylamine significantly enhances the hydrophilicity of biomaterials, hence effectively maximizing their biocompatibility.[12] Allylamine improves bioactivity by serving as an amine substrate that facilitates the attachment of biologically active proteins to the surfaces.[13,14] Prior research has shown that the existence of polar groups on the surface, particularly those abundant in nitrogen, promotes cellular adhesion.[15] Additionally, the plasma polymerized layer is biocompatible, integrates well with surrounding tissue cells, promotes antibacterial properties, and reduces chronic inflammation.[16]

Nevertheless, the utilization of bioactive amine organic compounds on zirconia ceramic biomaterials have limited research, further investigations is necessary. Therefore, this study was to examine the unique characteristics and reactivity of allylamine when applied to the surface of zirconia ceramics via GDP treatment, and its interaction with adjacent osteoblast cells.

Materials and methods

Zirconia ceramic samples preparation

The zirconia ceramic samples (Coho Technology, Taipei, Taiwan) underwent a process utilizing GDP in the presence of argon at 85 Watts (W) for 30 min, and then exposed to the amine compound in a GDP reactor (AST Products Inc., Billerica, MA, USA) as shown in Fig. 1. Three distinct circumstances were applied: 50W, 75W, or 85W, using 13.56 MHz and 100 millitorrs for another 30 min. These conditions are referred to as A50, A75, and A85.

Surface morphology and composition analysis

The scanning electron microscope (SEM; SU-3500; Hitachi Ltd., Kyoto, Japan) was used to observe surface morphology at 60× and 1,000× magnification, with an accelerating voltage of 20 kV in vacuum mode.

To identify the elemental composition of the zirconia surface, elemental energy-dispersive spectroscopy (EDS; SU-3500; Hitachi Ltd.) and X-ray photoelectron spectroscopy (XPS; PHI Quentera II, Ulvac-PHI Inc, Kanagawa, Japan) analysis were used. In EDS, the interaction of the electron beam with the sample generates characteristic X-

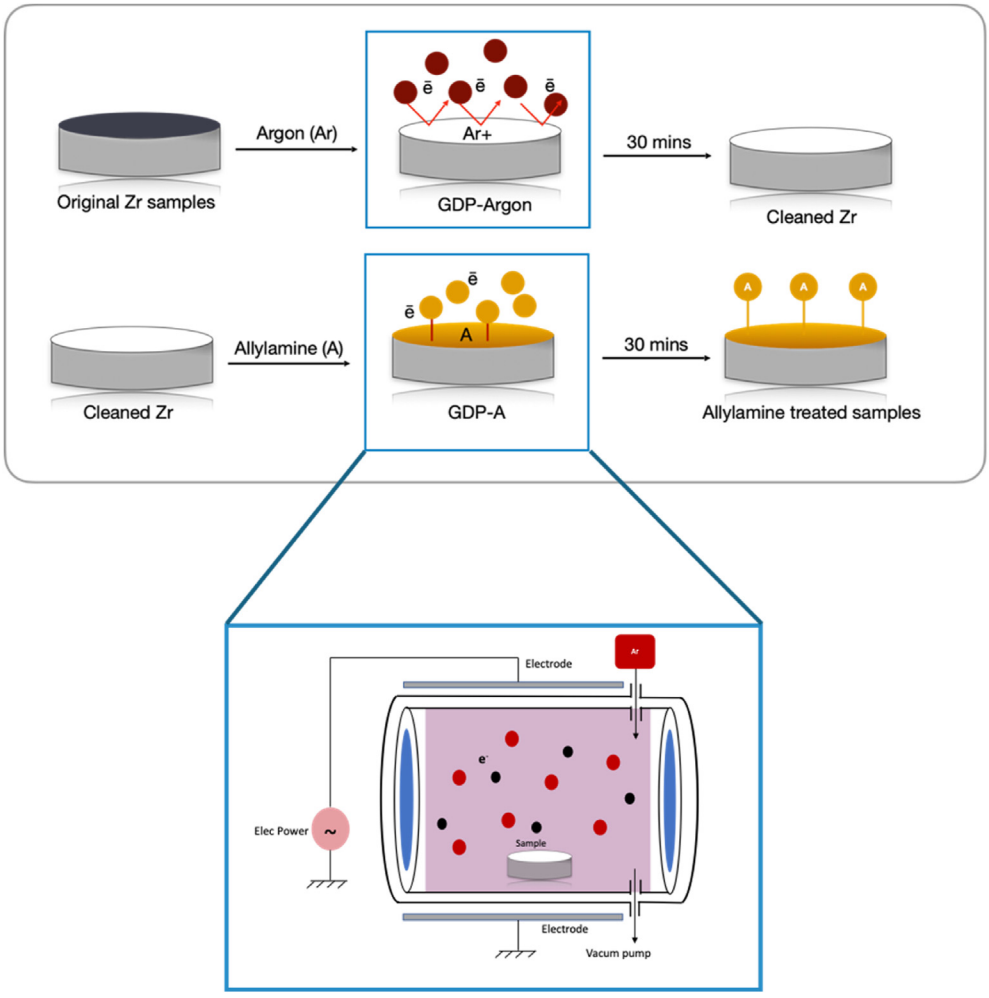

Figure 1 Illustration of a flowchart for glow discharge plasma (GDP) treatment and amine organic compound grafting. Zr indicates zirconia.

rays, producing a spectrum that reveals the surface's elemental composition. In XPS, the samples' surfaces were irradiated with monochromatic X-rays from an aluminum (Al Kα) source. The X-rays cause photoelectrons to be emitted from the surface atoms, which were then collected and analyzed by the electron energy analyzer.

Functional group analysis

Fourier-transform infrared spectroscopy (FTIR; Nicolet iS5 instrument, Thermo Fisher Scientific, Waltham, MA, USA) was used to analyze the functional groups of test samples in this study. The prepared samples were placed in contact with the attenuated total reflectance (ATR) crystal. Infrared (IR) light was directed into the ATR crystal, where it underwent multiple internal reflections, creating an evanescent wave that interacts with the surface molecules. This allows for the absorption of wavelengths ranging from 3650 to 650 cm−1, which characterizes the different chemical bonds.

Surface hydrophilicity and roughness analysis

A 4 μL droplet of ultra-pure water (Millipore-Q system, Merck Millipore, Burlington, MA, USA) was dispensed onto the zirconia disk's surface, and the droplet profile was captured by a contact angle meter (GBX Digidrop, GBX Scientific LTD, Dublin, Ireland) to measure surface hydrophilicity. The contact angle was calculated from multiple measurements taken at three different locations to ensure accuracy. Surface roughness measurements were conducted using an atomic force microscope (AFM) (Nanoview 1000, FSM Precision Inc, Suzhou, China). Samples were prepared by depositing graphene nanosheets onto mica surfaces using a drop-casting method and analyzed in tapping mode.

Cell viability and cell adhesion analysis

MG-63 human osteoblast-like cells were acquired from the Cell Cultures of the Bioresource Collection and Research Centre (Hsinchu, Taiwan) and cultured in Dulbecco's

Table 1 Forward and reverse primer sequences of glyceraldehyde-3-phosphate dehydrogenase (GAPDH), alkaline phosphatase (ALP), osteocalcin (OC), distal-less homeobox 5 (DLX5), transcription factor SP7 (SP7), osteoprotegerin (OPG), and receptor activator of nuclear factor κ B (RANK).

Gene Symbol	Forward primer sequence (5'-3')	Reverse primer sequence (5'-3')
GAPDH	AAAAACCTGCCAAATATGAT	CAGTGAGGGTCTCTCTCTTC
ALP	CTTGTGCCTGGACGGACCCT	TGGTGCACCCCAAGACCTGC
OC	GCCCTCACACTCCTCGCCCTATT	GGGTCTCTTCACTACCTCGCTGCC
DLX5	CAACTTTGCCCGAGTCTTC	GTTGAGAGCTTTGCCATAGG
SP7/OSX	TGGCGTCCTCCCTGCTTG	TGCTTTGCCCAGAGTTGTTG
OPG	GAAGGGCGCTACCTTGAGAT	GCAAACTGTATTTCGCTCTGG
RANK	TGTGGCACTGGATCAATGAG	GTCTTGCTGACCAATGAGAG

Modified Eagle's Medium (DMEM; Merck KGaA Inc, Darmstadt, Germany) supplemented with 10% fetal bovine serum (FBS; Thermo Fisher Scientific, San Jose, CA, USA) under humidified condition with 5% CO_2 at 37 °C.

Cell viability was assessed using the 3-(4,5-Dimethylthiazol-2-yl)-2,5 Diphenyltetrazolium Bromide (MTT) assay kit (Roche Applied Science, Mannheim, Germany) on 1, 3, 5, and 7 days. MTT working solution was added, followed by incubation for 2 h. The formazan crystals were then dissolved with DMSO, and absorbance was measured at 570 nm using a microplate reader (SpectraMax iD3, Molecular Devices LLC, San Jose, CA, USA). The cell adhesion was observed by immunofluorescent assay. Briefly, the cells were fixed with 4% paraformaldehyde, permeabilized with 0.1% Triton X-100, blocked with 1% BSA. Cells were then stained with Alexa Fluor 488-phalloidin (Invitrogen, Waltham, MA, USA) and DAPI (Sigma–Aldrich, St. Louis, MO, USA), and visualized using a confocal laser scanning microscope (Leica Microsystem, Wetzlar, Germany).

Cell differentiation and mineralization analysis

In alkaline phosphatase (ALP) assay (BioVision, Exton, PA, USA), cells were cultured for 1, 3, 5, and 7 days. 500 μL of cell lysates were mixed with assay buffer and incubated with p-nitrophenyl phosphate (pNPP) substrate at 37 °C for 2 h, and absorbance was measured at 405 nm. Mineralization activity was analyzed at 7, 14, and 21 days. Cells were fixed with 70% ethanol for 1 h, washed and stained with Alizarin Red S solution (Sigma–Aldrich) for 10 min. The dye was extracted with 10% acetic acid and measured at 540 nm.

Osteoblast related gene expression analysis

The gene expression of alkaline phosphatase (ALP), osteocalcin (OC), distal-less homeobox 5 (DLX5), transcription factor SP7 (SP7), osteoprotegerin (OPG) and receptor activator of nuclear factor κ B (RANK) was measured by reverse transcription-quantitative polymerase chain reaction (RT-qPCR) following the protocol described in the previous study.[17] In brief, 1 μL of Trizol (Thermo Fisher) was used to extract RNA and mixed with chloroform. The mixture was centrifuged at 4 °C for 30 min at 15,000 rpm after isopropanol was added. After the mRNA was converted cDNA, quantitative PCR was performed by using Fast SYBR™ Green Master Mix (Thermo Fisher) and analyzed with LightCycler Instrument (Roche Molecular Systems, Pleasanton, CA, USA). The list of primer sequences is provided in Table 1.

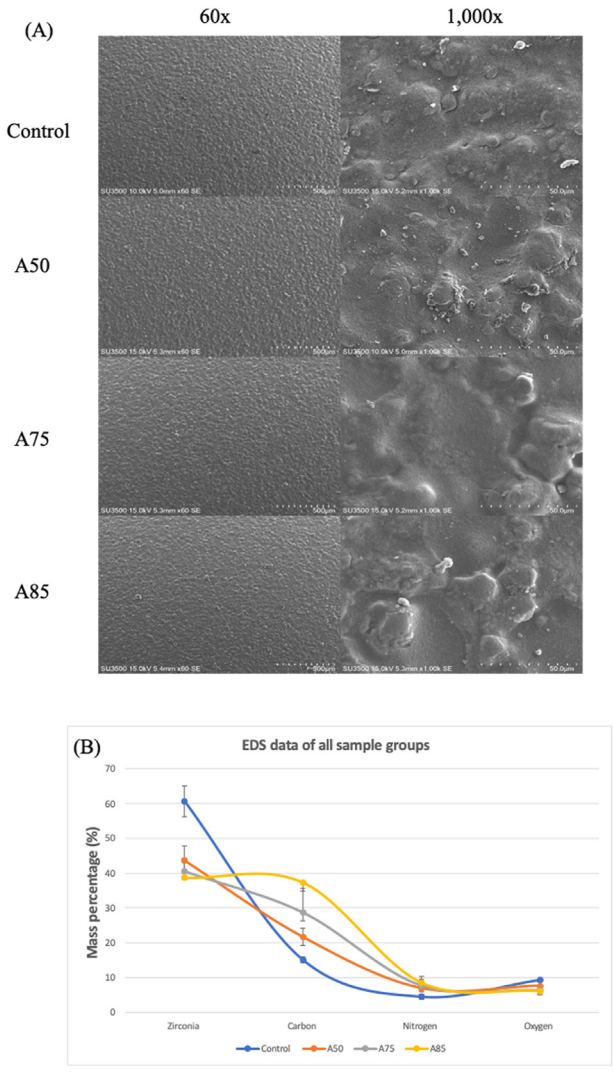

Figure 2 (A) The surface morphology of samples under scanning electron microscopy (SEM) observation. (B) Line graph of surface components by energy dispersive spectroscopy (EDS) analysis.

Statistical analysis

The data from the experimental analyses were described using means and standard deviations. Data were compared using two-way analysis of variance (ANOVA), Tukey multiple comparison test, and correlation. Simple linear regression was used for multiple comparisons among different groups. Statistical analyses were performed using Prism (v10; GraphPad Software Inc., Boston, MA, USA). Values of $P < 0.05$ were considered statistically significant.

Results

Examination of surface morphology

The SEM images revealed that control zirconia disk exhibited a smoother surface compared to other surface-treated disks (Fig. 2A). Significantly, the allylamine-treated samples exhibited irregular bulbous patterns on their surface, which were particularly pronounced at 1000 x magnification. When the GDP allylamine wattage increased from A50 to A85, the rounded bulbous patterns and surface deposits became more noticeable.

Analysis of surface composition

EDS results showed that control zirconia had the lowest carbon (C) and nitrogen (N) content while having the highest oxygen (O) concentration (Fig. 2B). Allylamine-treated samples exhibited increased levels of C and N as the GDP wattage elevated. XPS analysis showed that the C, N, and O content of the control zirconia disk were 57.74% (±17.8), 1.81% (±0.51), and 29.5% (±13.7), respectively. The C and N contents of all allylamine-treated groups were higher compared to the control zirconia disk (Fig. 3A).

FTIR functional groups analysis

The samples treated with allylamine exhibited the presence of aromatic C—H, C—O stretching, N—H stretching, C^C, and C—H bonds (Fig. 3C). The data indicated that with increasing concentration of allylamine, the visibility of these functional groups became more pronounced, and the intensity of absorption bands increased compared to the untreated zirconia sample.

Measurement of surface hydrophilicity and roughness

The water droplets contact angle on the surface of the untreated zirconia disk is 72.03° (±3.61°) while 31.80° (±2.81°) for A50, 40.30° (±0.96°) for A75, and 53.53° (±1.78°) for A85 (Fig. 4A and B). There was a statistically significant difference between the control and allylamine-treated groups. The control zirconia disk had an average roughness (Ra) value of 0.76703 ± 0.1810 μm. After allylamine treatment, Ra vale elevated to 1.0090 ± 0.5007 μm (A50), 1.7691 ± 0.6627 μm (A75), and 2.0774 ± 0.6615 μm (A85). Significant differences were found only for A85 group when compared with control and A50 group. The 3D surface roughness illustration is shown in Fig. 4E and F.

Cell viability and cell adhesion analysis

On day 3 and day 5, the A50 group exhibited the highest MG-63 cell viability, reaching 183% and 193%, respectively, with

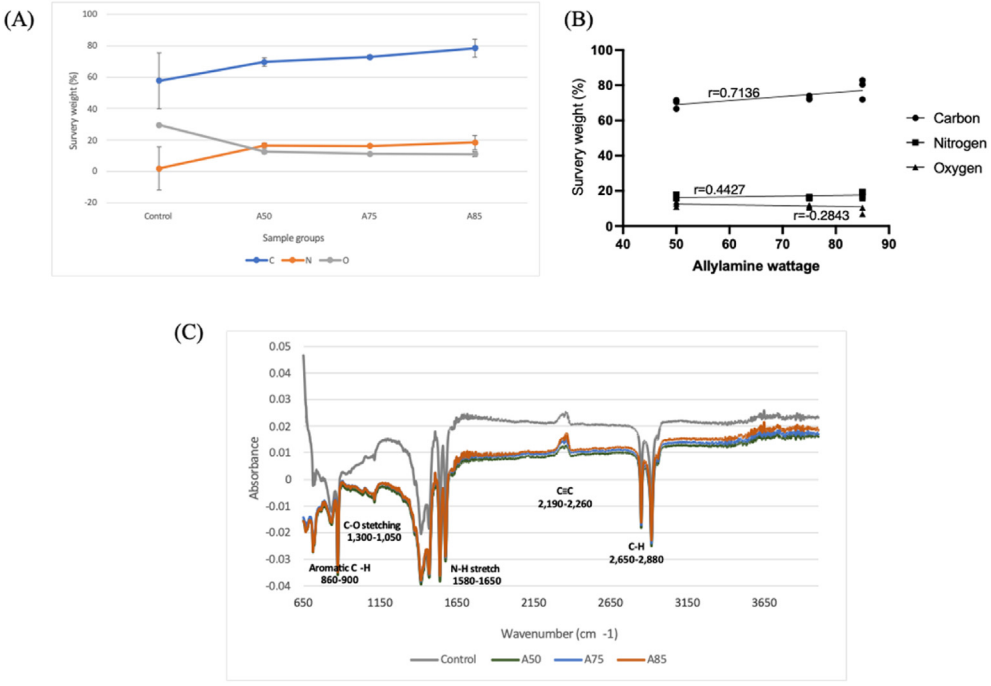

Figure 3 (A) Line graph of surface configuration by X-ray photoelectron spectroscopy (XPS), (B) Correlation coefficient between allylamine wattage and C, N and O weight percentage, and (C) Atomic peaks and functional groups analysis by Fourier transform infrared spectroscopy (FTIR).

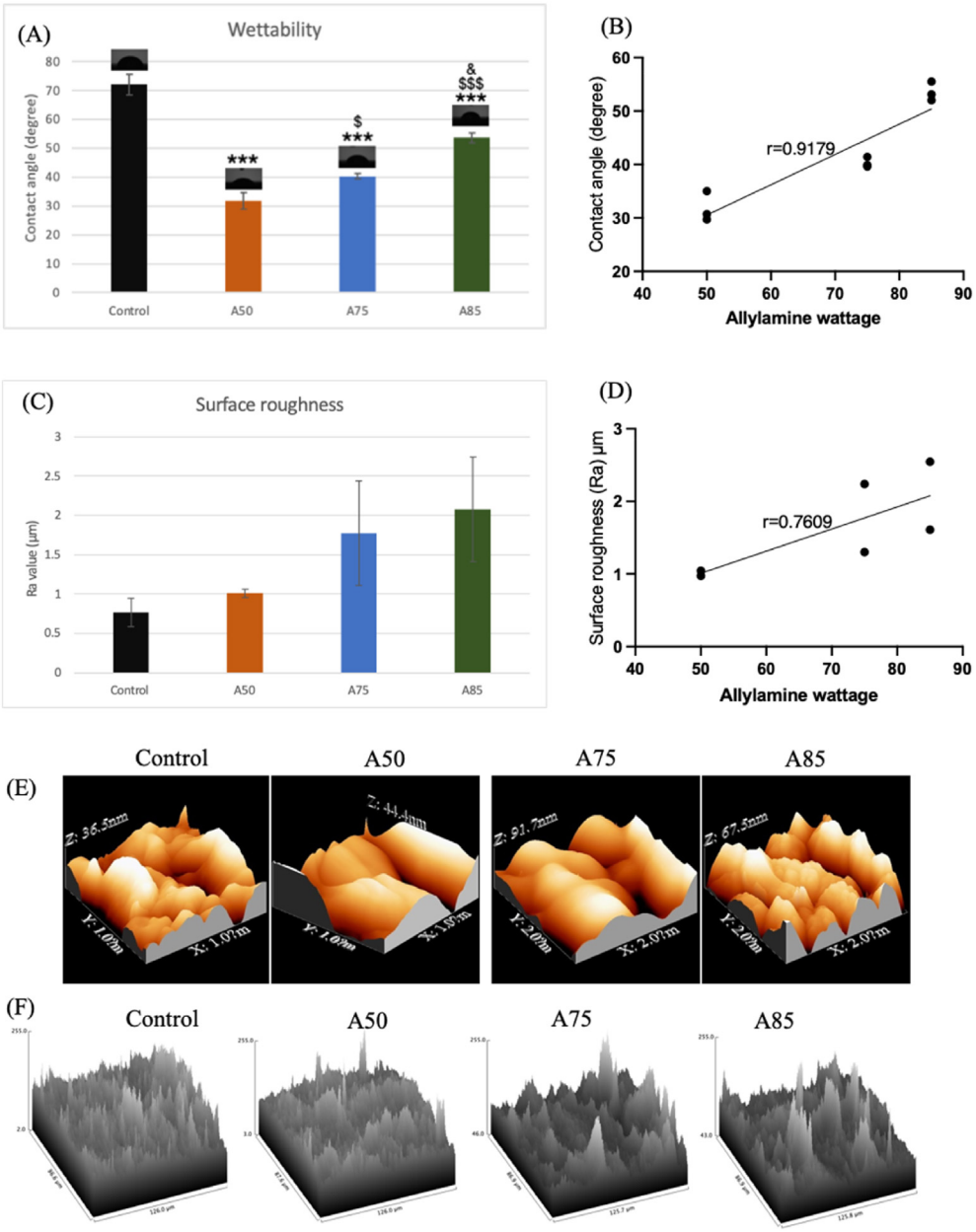

Figure 4 (A) Surface hydrophilicity analyzed by contact angle meter. (B) Correlation coefficient between contact angle and concentration of allylamine. (C) Surface roughness analysis by atomic force microscopy (AFM). (D) Correlation coefficient between increased amine concentration and surface roughness. (E–F) Surface roughness for each sample in 3D images. Significant difference compared with control is indicated with * $P < 0.05$, ** $P < 0.01$ and *** $P < 0.001$, while $^{\$}$ symbol for comparing with A50, and $^{\&}$ symbol used for comparison with A75.

all allylamine-treated groups showing significantly higher viability than the control. By day 7, the A50 group maintained the highest viability at 270%, followed by A75 at 195% and A85 at 183% (Fig. 5A). The cell adhesion analysis showed that MG-63 cells began to grow and firmly adhere to the zirconia surface within 12 h, and demonstrate the osteoblast-like robust adhesion to the zirconia surface after 24 h.

Cell differentiation and mineralization analysis

The ALP enzyme activity increased by the 7th day (Fig. 6). The A50 group exhibited the highest enzyme expression level among all groups, with a value of 0.6203 U/L. The A85 group recorded 0.5548 U/L on day 7, while the A75 group had the second-highest value of 0.5617 U/L. Significant

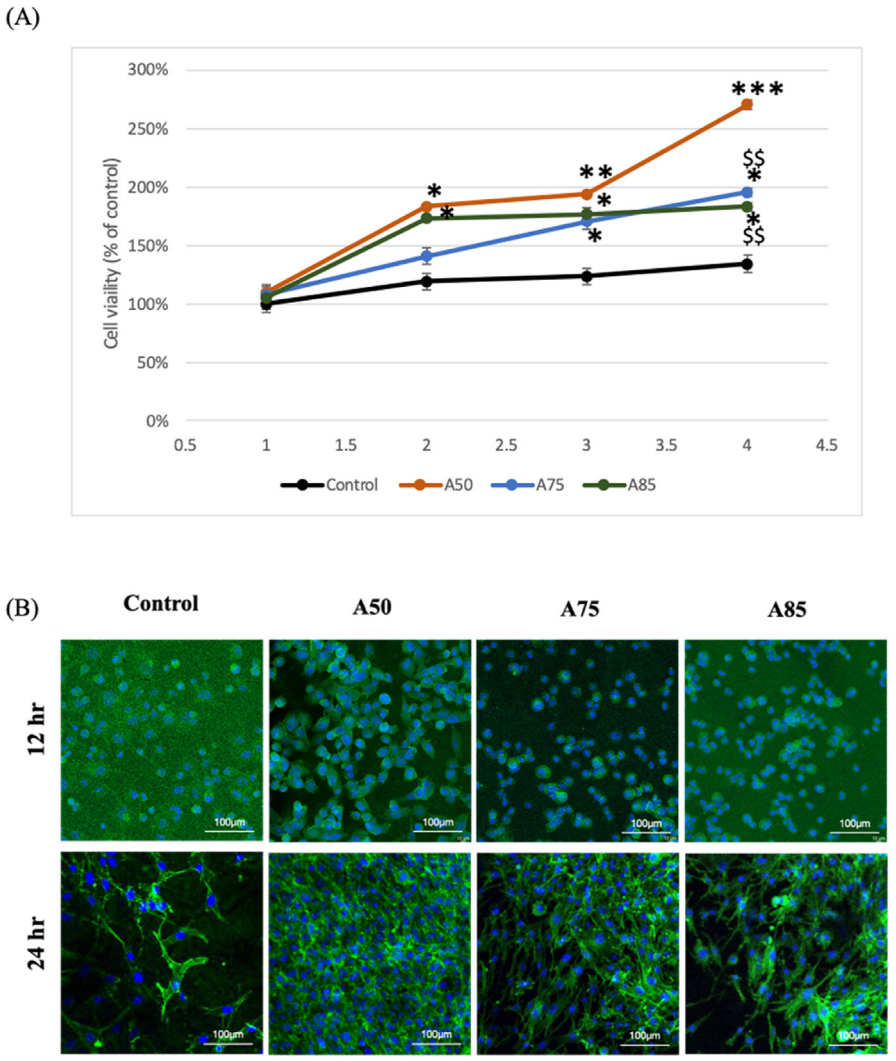

Figure 5 (A) Cell viability from day 1 to day 7 by MTT assay. Significant difference compared with control is indicated with * $P < 0.05$, ** $P < 0.01$ and *** $P < 0.001$, while $^{\$}$ symbol for comparing with A50. (B) Immunofluorescent assay of cell adhesion at 12 and 24 h.

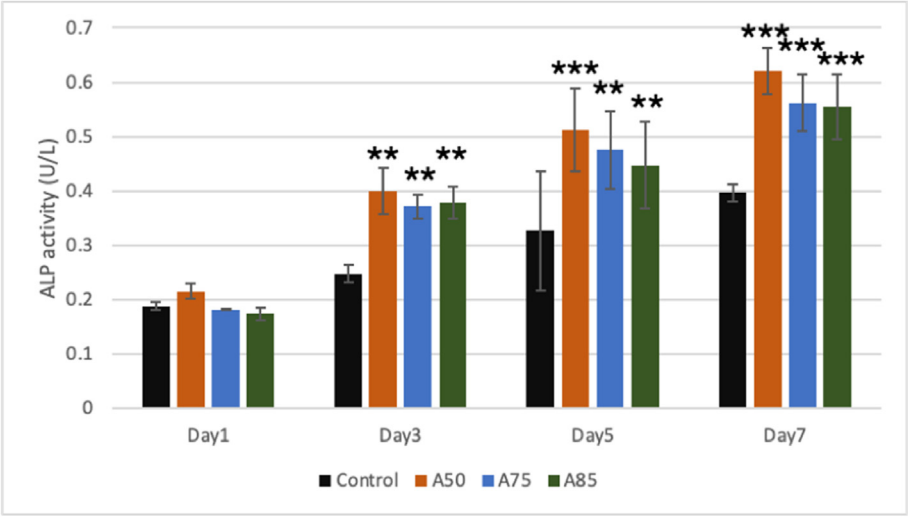

Figure 6 Alkaline phosphatase (ALP) enzyme activity from day 1 to day 7. Significant difference compared with control is indicated with * $P < 0.05$, ** $P < 0.01$ and *** $P < 0.001$.

differences were observed between the control and allylamine-treated groups from day 3 to day 7. Qualitative and quantitative evaluations of calcium (Ca) deposition in the extracellular matrix showed that the A50 and A75 groups had the highest Ca content at day 14 and day 21, Furthermore, there was a statistically significant difference between A50 groups and the control disk on day 21 (Fig. 7).

Osteogenic gene expression analysis

The expression levels of osteogenic gene markers demonstrated a gradual increase over the cultivation period (Fig. 8). On day 14 and 21, the A50 exhibited the highest expression of all markers, except for OPG, which was highest in the A85 group. Additionally, the SP7 and DLX5 markers increased initially until day 7 but began to decline by day 14. On day 21, ALP levels showed a statistically significant difference between the A50 and A85 groups, while OC levels were significantly different between the A50 group and both A75 and A85 groups.

Discussion

In our study, the SEM observation validated the effective grafting of amine compounds onto the zirconia samples. Both EDS and XPS analyses show a progressive increase in carbon and nitrogen elements as the wattage of allylamine

(A)

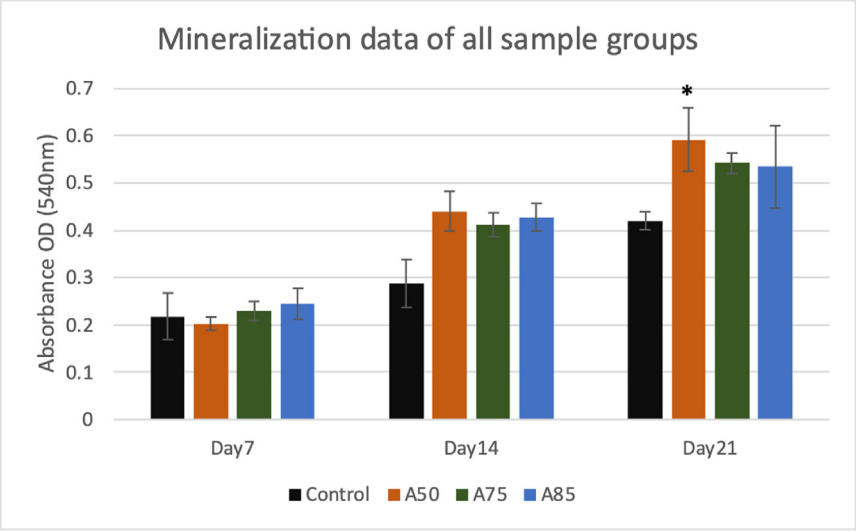

(B)

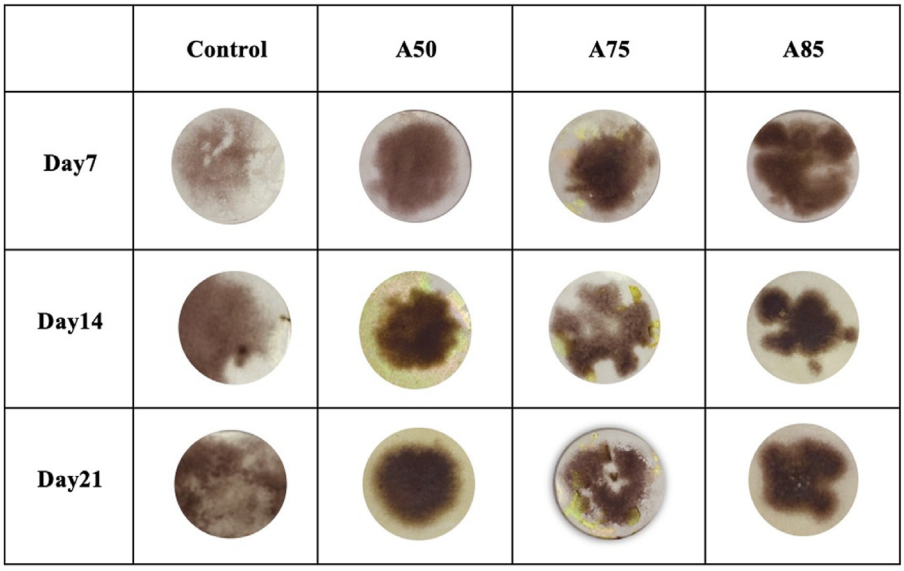

Figure 7 (A) Boxplot of mineralization capability (late-stage markers) of osteoblasts on allylamine-treated groups. Significant difference compared with control is indicated with * $P < 0.05$. (B) Alizarin red S-stained images of sample groups from day 7, day 14 day 21.

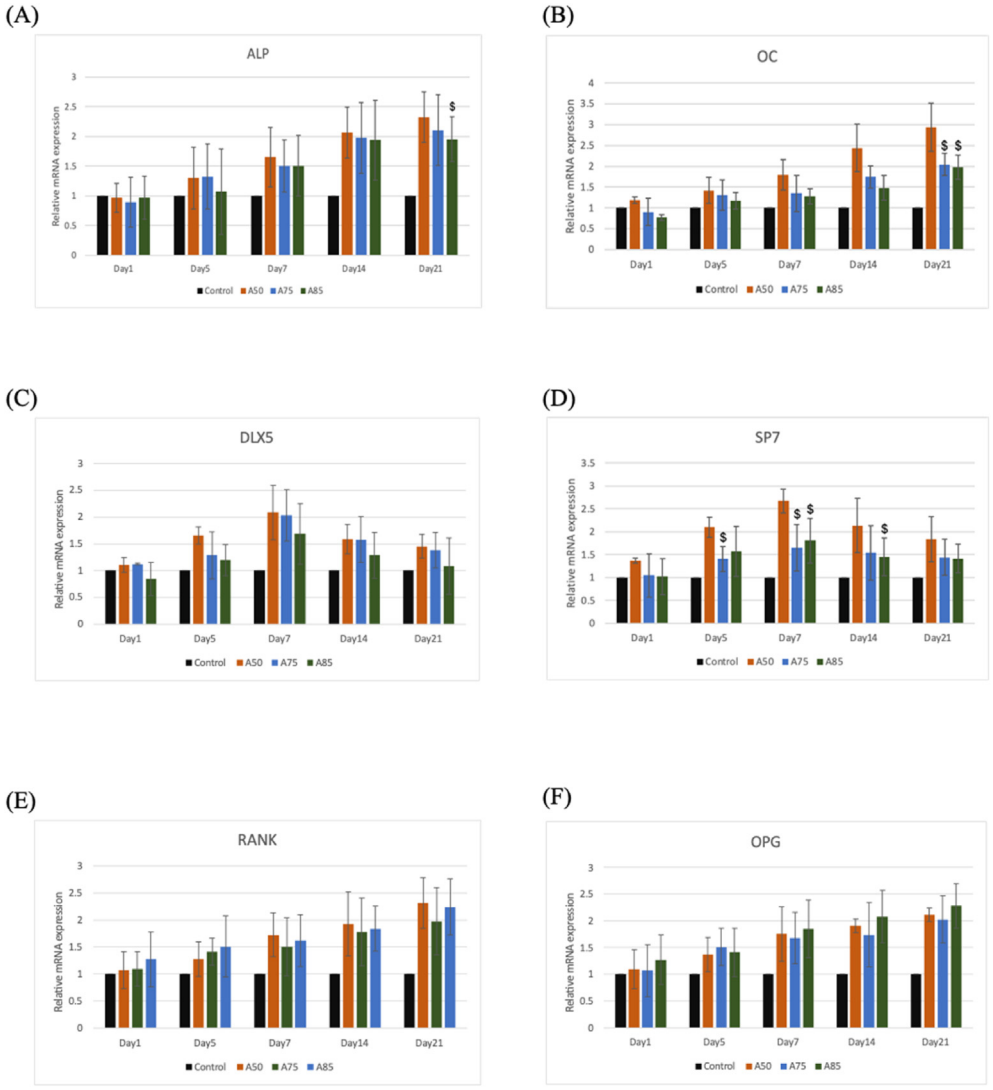

Figure 8 The expression of osteogenic related gene by reverse transcription-quantitative polymerase chain reaction (RT-qPCR) for (A) alkaline phosphatase (ALP), (B) osteocalcin (OC), (C) distal-less homeobox 5 (DLX5), (D) transcription factor SP7 (SP7), (E) receptor activator of nuclear factor κ B (RANK), and (F) osteoprotegerin (OPG). Significant difference compared with A50 is indicated with $^{\$}$, $P < 0.05$.

increases (Fig. 3B). The presence of allylamine, with the formula of $C_3H_5NH_2$, is evident due to the contribution of its carbon and nitrogen atoms.[18] Additionally, FTIR analysis determined the chemical bonds and functional groups present in the allylamine-treated groups, including aromatic C—H, C—O, N—H, and C ^ C bonds, which are attributed to its $C_3H_5NH_2$ chemical structure.

There is a significant correlation between contact angle and the concentration of allylamine (Fig. 4B). Lower concentrations of allylamine result in lower contact angles and improved hydrophilicity. Increased allylamine concentration leads to a more textured surface. One *in vitro* research by Gavilán et al., has demonstrated that the roughness of a biomaterial can impact the initial development and metabolism of cells, ultimately enhancing clinical outcomes.[19] Our modifications resulted in a surface Ra value of 1.009 to 2.077 μm, compared to the control ceramic's Ra of 0.7670 μm. A moderate correlation (r = 0.7609) exists between increasing allylamine concentration and surface roughness (Fig. 4D). Allylamine treatment enhances roughness, which in turn boosts osteoblast activity and bone apposition. Fischer et al. reported a similar Ra of 1.2 μm after sandblasting with alumina and hydrofluoric acid etching.[6] Additionally, a classical paper by Albrektsson and Wennerberg found that a Ra of 1—2 μm promotes optimal osseointegration, which aligns with our roughness data around 2 μm.[20]

The MTT assay indirectly assesses cell vitality, growth, and mitochondrial function.[21] On day 7, the A50 group had the highest cell viability, followed by A75 and A85. This result supports Wanqi Yu's study, which found greater MG-63 cell proliferation and adherence on a plasma-enhanced chemical vapor-coated surface.[22] The increased proliferation may be attributed to enhanced cell adhesion and

spreading observed at 12 and 24 h in allylamine-treated samples, due to the cell-attractive properties of the amine groups. Kunz et al. also showed that osteoblasts benefit from the positive charges of a plasma-polymerized amine layer, despite reduced spreading ability.[23]

Following the initial 12-h cultivation period (Fig. 5B), MG-63 cells showed greater adhesion and proliferation on allylamine-treated samples. The A50 group exhibited the highest cell growth at both 12 and 24 h, eventually covering the entire surface. Afterwards, phosphatase activity and calcium mineralization, key markers of osteoblast development and bone mineralization were conducted (Figs. 6 and 7), and the A50 group had the highest ALP activity and calcium deposits compared to the other groups. Tang et al. similarly found that UV-exposed TiO_2-modified zirconia promoted cell proliferation, increased ALP activity, and enhanced mineralization.[24]

The gene expression markers aligned with cell differentiation and proliferation results, which were evaluated in this study. ALP, an early osteogenic marker,[25] and OC, which is associated with the bone formation process, were both elevated. DLX5 and SP7, early-stage osteoblast differentiation markers,[26] showed upregulation until day 7 before downregulating. Elevated levels of RANK and OPG on day 7 indicate substantial bone remodeling, which is essential for the production of new osteoblast cells and bone.[27] Nishizaki et al. demonstrated that a nanostructured zirconia/alumina composite implant improved ALP activity and osteogenic gene expression.[28] Similarly, Chaves et al. achieved increased osteogenic differentiation of stem cells derived from adipose tissue by polymerizing amines through plasma treatment.[29] However, the study still has some limitations associated with plaque adhesion and soft tissue integration properties. It should be further investigated in future research.

The properties of zirconia ceramics were significantly enhanced by combining amine compounds with surface modification using GDP. Both surface hydrophilicity and roughness of the zirconia ceramic were notably improved after surface modification. Most importantly, amine grafting markedly enhanced the material's bioactivity, improving cell viability, differentiation, and osteogenic properties, thereby overcoming zirconia's inherent bioinertness. The optimal outcomes were observed with the allylamine 50- Watts group. These findings open new avenues for enhancing the performance of zirconia-based implants, potentially leading to better clinical outcomes in dental implants and orthopedic applications.

Declaration of competing interest

The authors have declared that there are no competing interests.

Acknowledgements

This research was funded by the National Science and Technology Council of Taiwan, NSTC 112-2221-E-038-006-MY3, and Taipei Medical University-National Taiwan University of Science and Technology Joint Research Program, Taiwan, TMU-NTUST-113-05

References

1. Rebl H, Finke B, Schmidt J, et al. Accelerated cell-surface interlocking on plasma polymer-modified porous ceramics. *Mater Sci Eng C* 2016;69:1116—24.
2. Totou D, Naka O, Mehta SB, Banerji S. Esthetic, mechanical, and biological outcomes of various implant abutments for single-tooth replacement in the anterior region: a systematic review of the literature. *Int. J. Implant Dent.* 2021;7:1—17.
3. Zhang Y, Lawn BR. Novel zirconia materials in dentistry. *J Dent Res* 2018;97:140—7.
4. Bona AD, Pecho OE, Alessandretti R. Zirconia as a dental biomaterial. *Materials (Basel)* 2015;8:4978—91.
5. Sivaraman K, Chopra A, Narayan AI, Balakrishnan D. Is zirconia a viable alternative to titanium for oral implant? A critical review. *J Prosthodont Res* 2018;62:121—33.
6. Fischer J, Schott A, Märtin S. Surface micro-structuring of zirconia dental implants. *Clin Oral Implants Res* 2016;27:162—6.
7. Chung SH, Kim HK, Shon WJ, Park YS. Peri-implant bone formations around (Ti,Zr)O_2-coated zirconia implants with different surface roughness. *J Clin Periodontol* 2013;40:404—11.
8. Caravaca CF, Flamant Q, Anglada M, Gremillard L, Chevalier J. Impact of sandblasting on the mechanical properties and aging resistance of alumina and zirconia based ceramics. *J Eur Ceram Soc* 2018;38:915—25.
9. Çağlar İ, Yanıkoğlu N. The effect of sandblasting, Er:YAG laser, and heat treatment on the mechanical properties of different zirconia cores. *Photomed Laser Surg* 2015;34:1726.
10. Suganya A, Shanmugavelayutham G, Rodríguez CS. Study on plasma pre-functionalized PVC film grafted with TiO2/PVP to improve blood compatible and antibacterial properties. *J Phys D Appl Phys* 2017;50:145402.
11. Yang CH, Li YC, Tsai WF, Ai CF, Huang HH. Oxygen plasma immersion ion implantation treatment enhances the human bone marrow mesenchymal stem cells responses to titanium surface for dental implant application. *Clin Oral Implants Res* 2015;26:166—75.
12. Chang YC, Feng SW, Huang HM, et al. Surface analysis of titanium biological modification with glow discharge. *Clin Implant Dent Relat Res* 2015;17:469—75.
13. Rohr N, Fricke K, Bergemann C, Nebe JB, Fischer J. Efficacy of plasma-polymerized allylamine coating of zirconia after five years. *J Clin Med* 2020;9:2776.
14. Khaled NI, Santhiya D. Multifunctional poly (allylamine hydrochloride)/bioactive glass layer by layer surface coating on magnesium alloy for biomedical applications. *Prog Org Coating* 2024;186:108059.
15. Sharifahmadian O, Zhai C, Hung J, et al. Mechanically robust nitrogen-rich plasma polymers: biofunctional interfaces for surface engineering of biomedical implants. *Mater Today Adv* 2021;12:100188.
16. Walschus U, Hoene A, Patrzyk M, et al. A cell-adhesive plasma polymerized allylamine coating reduces the in vivo inflammatory response induced by Ti6Al4V modified with plasma immersion ion implantation of copper. *J Funct Biomater* 2017;8:30.
17. Aung LM, Lin JC, Salamanca E, et al. Functionalization of zirconia ceramic with fibronectin proteins enhanced bioactivity and osteogenic response of osteoblast-like cells. *Front Bioeng Biotechnol* 2023;11:1159639.

18. O'Neill F, O'Neill L, Bourke P. Recent developments in the use of plasma in medical applications. *Plasma* 2024;7:284—99.
19. Romero-Gavilán F, Arias-Mainer C, Cerqueira A, et al. Roughness affects the response of human fibroblasts and macrophages to sandblasted abutments. *Biomed Eng Online* 2024;23:68.
20. Albrektsson T, Wennerberg A. Oral implant surfaces: part 1-review focusing on topographic and chemical properties of different surfaces and in vivo responses to them. *Int J Prosthodont (IJP)* 2004;17:536—43.
21. Van Meerloo J, Kaspers GJ, Cloos J. Cell sensitivity assays: the MTT assay. *Methods Mol Biol* 2011;731:237—45.
22. Yu W, Wang X, Guo Y, et al. The osteogenesis performance of titanium modified via plasma-enhanced chemical vapor deposition: in vitro and in vivo studies. *Biomed Mater* 2020;15:055012.
23. Kunz F, Rebl H, Quade A, Matschegewski C, Finke B, Nebe JB. Osteoblasts with impaired spreading capacity benefit from the positive charges of plasma polymerised allylamine. *Eur Cell Mater* 2015;29:177—88.
24. Tang S, Zhang J, Ding N, Zhang Z. Biological activity of titania coating prepared with zirconium oxychloride and titania on zirconia surface. *J Mech Behav Biomed Mater* 2021;123:104780.
25. Rutkovskiy A, Stensløkken KO, Vaage IJ. Osteoblast differentiation at a glance. *Med Sci Monit Basic Res* 2016;22:95—106.
26. Levi G, Narboux-Nême N, Cohen-Solal M. DLX Genes in the development and maintenance of the vertebrate skeleton: implications for human pathologies. *Cells* 2022;11:3277.
27. Bolamperti S, Villa I, Rubinacci A. Bone remodeling: an operational process ensuring survival and bone mechanical competence. *Bone Res* 2022;10:48.
28. Nishizaki M, Komasa S, Taguchi Y, Nishizaki H, Okazaki J. Bioactivity of NANOZR induced by alkali treatment. *Int J Mol Sci* 2017;18:780.
29. Chaves C, Alshomer F, Palgrave RG, Kalaskar DM. Plasma surface modification of polyhedral oligomeric silsequioxane-poly(carbonate-urea) urethane with allylamine enhances the response and osteogenic differentiation of adipose-derived stem cells. *ACS Appl Mater Interfaces* 2016;8:18701—9.